Inner Bremsstrahlung Emitted in Electron Capture Decay of Ni^{59}, A^{37}, and Fe^{55}†

BABULAL SARAF*
Bartol Research Foundation of The Franklin Institute, Swarthmore, Pennsylvania
(Received November 10, 1955)

The continuous gamma-ray spectra (inner bremsstrahlung) accompanying orbital electron capture in Ni^{59}, A^{37}, and Fe^{55} have been studied with the use of a scintillation spectrometer of NaI(Tl). The shape of the spectrum of Ni^{59} has been found to correspond to a second forbidden spectrum ($\Delta I=2$, No) and is distinctly different from that of an allowed one. The parameter, λ, of the correction factor, $C_{2s,T}$, is approximately 0.33; the value of A_{ij}/T_{ij}, for a pure tensor interaction, is (-6). The probability of emission of a photon of energy greater than 100 kev has been shown to be 1.4 ± 0.4 times the theoretical value.

The spectrum of A^{37} has an allowed shape at energies as low as $\sim$35 kev, and the ratio of emission probabilities $P_{(\text{exp})}/P_{(\text{theoret})}$ is 1.05 ± 0.25 for the region of energy lying above 35 kev. The spectrum of Fe^{55} has been compared with the calculations of Glauber and Martin. In this case, the value of $P_{(\text{exp})}/P_{(\text{theoret})}$ is 1.1 ± 0.3 at higher energies.

INTRODUCTION

THE inner bremsstrahlung of the electron capture process have been investigated in the case of several activities.[1–7] Since the experimentally observed spectra of Cs^{131}, Ge^{71}, and Fe^{55} have been shown[5–7] to be in disagreement with the early theory of Morrison and Schiff,[8] further theoretical studies have been carried out by Glauber and Martin.[9] Their calculations are in better agreement with experimental observations.

The spectra of A^{37} and Fe^{55} have been investigated previously.[1–5] It has been generally concluded that the characteristics of the spectrum of A^{37} are in good agreement with theory[8] in the energy region extending from 300 kev to the end point. The spectrum of Fe^{55} has been studied by Madansky and Rasetti.[5] At quantum energies below $\sim$30 kev, a sharp rise in intensity was enountered which is similar in nature to the effects observed[6,7] in Cs^{131} and Ge^{71}. From a consideration of the lifetime of the decay (8×10^4 yr) and the ground-state orbitals of Ni^{59} ($p_{3/2}$) and Co^{59} ($f_{7/2}$), as predicted by the shell model, the transition is expected to be second forbidden. In the measurements of Emmerich *et al.*,[4] no significant deviation of spectral shape from that of an allowed transition was observed in the energy interval extending from 300 kev to 1060 kev.

In the present investigations, the gamma-ray spectrum of Fe^{55} has been compared with the calculations of Glauber and Martin[9] who have chosen more exact wave functions for the electrons than the plane waves of earlier calculations. They have also calculated the extent of contributions resulting from the capture of the s- and p-electrons of the L-shell.

The probability of radiative capture has been measured in the case of the three elements under discussion in this paper. Special attention has been given to determination of the detection efficiency of the crystal for the continua, taking into account source volume, etc. The actual disintegration rates were determined by noting the number of K-capture events in a proportional counter.

NICKEL-59

The half-period[10] of Ni^{59} is approximately 8×10^4 years. It is therefore difficult to obtain a source of sufficient specific activity that the inner bremsstrahlung spectrum can be readily studied. If naturally occurring nickel is irradiated by thermal neutrons, two long-lived activities, Ni^{59} and Ni^{63}, are produced. The decay of Ni^{63} proceeds with emission of negatrons of end-point energy 65 kev. No gamma rays are associated with this activity. In order to investigate the low energy region of the gamma-ray continuum of Ni^{59}, it is necessary to reduce to a minumum the amount of Ni^{63} present, since the bremsstrahlung associated with the beta rays might interfere with the measurements. With this fact in mind, a sample of nickel, enriched in Ni^{58} to the extent of 99.94%, was obtained from the Isotopes Division of the U. S. Atomic Energy Commission at Oak Ridge. This material was irradiated in the Arco pile for a time of 15 days. The resulting source contained several activities other than Ni^{59}, e.g., Co^{58}, so that a thorough chemical purification was necessary. Practically all the active impurities were removed by precipitations with various carriers such as Fe, Co, Cu, etc. Finally, Ni was precipitated by addition of dimethylglyoxine. Five successive precipitations were performed, and the material was finally converted to NiO.

† Assisted by the joint program of the Office of Naval Research and the U. S. Atomic Energy Commission.
* Research Fellow, Bartol. Present address: Department of Atomic Energy, Government of India, Apollo Pier Road, Bombay 1, India.
[1] H. Bradt *et al.*, Helv. Phys. Acta **19**, 222 (1946).
[2] D. Maeder and P. Preiswerk, Phys. Rev. **84**, 595 (1951).
[3] C. A. Anderson and G. W. Wheeler, Phys. Rev. **90**, 606 (1953).
[4] Emmerich, Singer, and Kurbatov, Phys. Rev. **94**, 113 (1954).
[5] L. Madansky and F. Rasetti, Phys. Rev. **94**, 407 (1954).
[6] B. Saraf, Phys. Rev. **94**, 642 (1954).
[7] B. Saraf, Phys. Rev. **95**, 97 (1954).
[8] P. Morrison and L. I. Schiff, Phys. Rev. **58**, 24 (1940).
[9] R. J. Glauber and P. C. Martin, Phys. Rev. **95**, 572 (1954).
[10] Brosi, Borkowski, Conn, and Griess, Phys. Rev. **81**, 391 (1951).

The radioactive source used for the study of the inner bremsstrahlung of Ni^{59} was formed by pressing 743 mg of powdered NiO into an aluminum ring of inner diameter 1.8 cm and thickness 0.3 cm, which was covered on either side with aluminum foil of thickness 7 mg/cm^2. A cylindrical crystal of NaI(Tl), 3.5 cm in diameter and 3.5 cm in height, was used for detection of the gamma-ray spectra. The source of Ni^{59} was placed at a distance of 2 mm from the crystal surface, coaxial with the crystal itself. Absorbing thicknesses of 35 mg/cm^2 of Al_2O_3 and 23 mg/cm^2 of Be intervened between the source and the crystal. The pulse-height spectrum of the inner bremsstrahlung of Ni^{59}, as observed in this geometry, is shown in Fig. 1, curve A. Most of the experimentally obtained points have a statistical accuracy of two to three percent, except near the end point where the statistical errors become as great as 6%. In computing the probable errors, the presence of the background count was properly taken into account.

The theoretical investigations of Glauber and Martin[9] and the experimentally observed shapes of the spectra[4–7] of Cs^{131}, Ge^{71}, Fe^{55}, and A^{37} show that deviations of spectral shape from the allowed form of

$$N(x) \propto x(1-x)^2, \quad x=E/E_0,$$

where E is the quantum energy, and E_0 the total disintegration energy, occur only in the region of energies near that of the K x-rays. According to the evidence cited above, the spectral distribution to be expected for Ni^{59} would be proportional to $x(1-x)^2$ in the region of energy extending from ~50 kev to the end point at 1060 kev. Emmerich, Singer, and Kurbatov[4] have investigated the shape of the gamma-ray spectrum of Ni^{59} in the interval of energy between 320 kev and the end point, finding no deviation from the expected distribution. With the aforementioned theoretical and

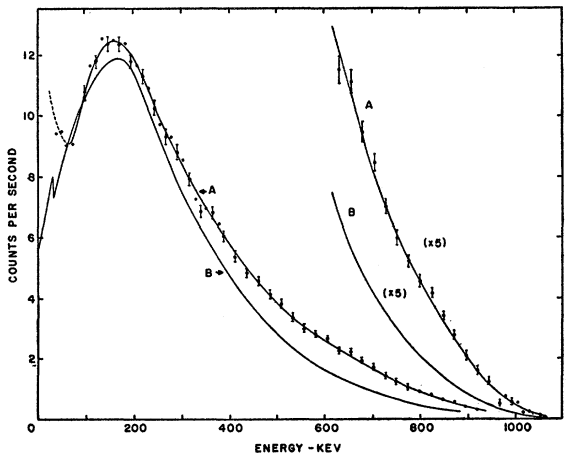

FIG. 1. Curve A, observed plus-height distribution of the gamma rays of Ni^{59}. Curve B, theoretical shape of the allowed transition for an end-point energy of 1060 kev, modified to take into account the experimental conditions.

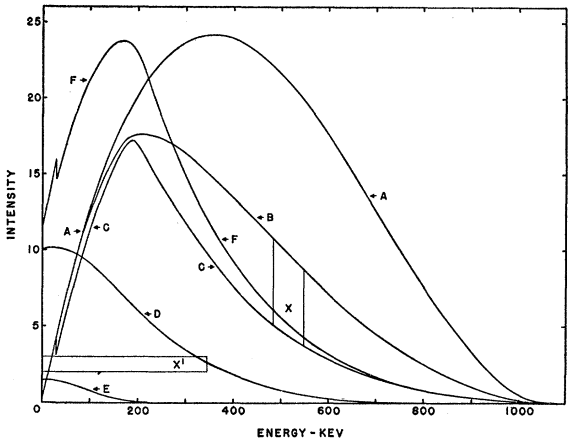

FIG. 2. Modification of the theoretically predicted spectral shape for Ni^{59} to resemble that expected to be observed. For details, see text.

experimental results in mind, a detailed comparison of the gamma-ray distribution of Ni^{59} with the expression $x(1-x)^2$ has been carried out. The measurements have been extended to very low quantum energies, and a comparison of the observed spectrum of Ni^{59} with the form $x(1-x)^2$ has been effected. Such a comparison can be made by distorting the theoretically expected spectrum to take into account the experimental conditions; or conversely, the experimentally determined distribution can be corrected for the effects of the various absorption processes and geometrical factors which are encountered in the course of detection of the quantum radiations. In analyzing the results under discussion in this paper, both types of analysis have been carried out.

The procedure for working out the experimentally observable pulse-height distribution from the theoretically calculated spectrum for Ni^{59} is illustrated in Fig. 2. The theoretically obtained spectrum for an allowed transition of the form $x(1-x)^2$ is represented by curve A, assuming an end-point energy for Ni^{59} of 1060 kev. The same distribution, corrected for variation of detection efficiency as a function of quantum energy, is shown as curve B. The spectral intensities of curve B have been decomposed into two curves to show full-energy absorption and Compton absorption. The resulting distributions are shown in curves C and D. The area under curve C has been properly reduced to take into account escape of the x-rays of iodine. The contribution resulting from x-ray escape to the region of low energy is shown in curve E. The final pulse-height spectrum is shown in curve F. In altering, as in the foregoing, the theoretically expected spectrum to conform to the experimental conditions, the Gaussian distribution of pulse heights relating to a single quantum energy has not been taken into account. This correction has been adjudged significant only in the region of the iodine escape peak and near the end point of the

spectrum. In the particular counting arrangement employed, the full-energy peak of the 662-kev gamma ray had a full width at half-maximum of 8% in energy. The following paragraphs describe in more detail the operations performed to obtain the curves of Fig. 2.

In order to determine how the detection efficiency of the crystal varied with quantum energy for the source geometry employed, a series of careful measurements were performed wherein monoenergic gamma-ray emitters such as Tl^{202} (430 kev), Cs^{137} (662 kev), Co^{58} (810 kev), etc., were studied over the volume of the source. The detection efficiencies were determined by moving point sources along the axis perpendicular to the face of the crystal and outward from the same axis radially. The variations with energy of the over-all efficiency for detection of radiation emitted from the entire source volume was found to be within 3% of that of a point source at a distance of 0.4 cm from the crystal surface and on the axis of the crystal. The energy-dependent crystal detection efficiency for a point source on the axis of the crystal is given by

$$\epsilon_E=\frac{1}{(1-\cos\beta)}\left[\int_0^{\alpha}\sin\theta(1-e^{-\mu_E L\sec\theta})d\theta + \int_{\alpha}^{\beta}\sin\theta(1-e^{-\mu_E(b\csc\theta-d\sec\theta)})d\theta\right],$$

where L is the crystal length, $2b$ the crystal diameter, d the source to crystal surface distance, and μ_E the linear absorption coefficient in NaI(Tl) for a gamma ray of energy E. The angles α and β are, respectively, $\tan^{-1}[b/(d+L)]$ and $\tan^{-1}(b/\alpha)$. This integral has been graphically evaluated and the results are shown in Fig. 3. The detection efficiencies so deduced have been employed in obtaining curve B of Fig. 2.

The ratio of the number of pulses in the full-energy absorption peak to the total number of pulses of all sizes generated in the crystal has been previously determined[6] at a number of gamma-ray energies for the particular crystal dimensions employed in these measurements. For a given gamma-ray energy, the value of this ratio was found to remain unchanged over the source volume. The ordinates of curve B of Fig. 2 were multiplied by this ratio to obtain curve C of the same figure. The area included between curves B and C has been redistributed in the form of Compton contributions to give curve D. The transformation of area X into area X' is indicated in Fig. 2. The length of the strip X' is determined by the maximum energy of the Compton recoil electron which can be knocked on by a quantum having the mean energy of the strip X. Observation of pulse height distributions arising from the monoenergic gamma rays of Mn^{54} (840 kev), Cs^{137} (662 kev), Ru^{103} (498 kev), Tl^{202} (430 kev), and Cr^{51} (320 kev) have shown that the assumption of a rectangular shape for the Compton distribution is justified. Curve E of Fig. 2 follows from calculations for very poor geometry as given by Axel.[11] Curve F, the resultant of all of the above cited modifications of the theoretically expected distribution to conform to the experimental conditions, is shown as curve B in Fig. 1. A comparison of the shapes of curves A and B of Fig. 1 shows that if the observed and calculated spectral intensities are taken to be equal at low energies, a difference of as much as a factor of 2 develops at higher energies. Thus, there is definite evidence that the shape of the distribution for Ni^{59} differs from that of an allowed spectrum.

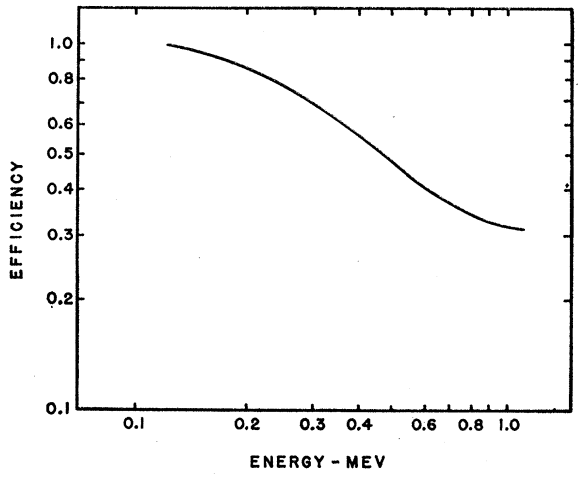

FIG. 3. Detection efficiency of the crystal as a function of quantum energy for a source distance of 0.4 cm along the crystal's axis.

It is of interest to obtain from the experimental observations the exact shape of the energy spectrum of the photons which are emitted in the decay of Ni^{59}. Before calculating the distribution it is necessary to consider to what extent the experimental observations may have been influenced by backscattering in the thick source itself. Compton scattering within the source will produce an appreciable number of pulses in the energy region extending from 150 kev to 300 kev. The number of pulses falling in this energy region were observed as the source backing was increased by adding successively three copper foils, each of thickness 120 mg/cm^2. The data were extrapolated to zero absorber thickness to obtain results free of the effects of backscattering. It was found that this correction attained a maximum of 3% at $\sim$200 kev.

To construct the energy distribution of the photons from the experimental observations, it is convenient to refer to the various curves shown in Fig. 2. Curve A, the observed distribution of Fig. 1, can be taken as corresponding to curve F of Fig. 2. In Fig. 2, it is seen that curve C and curve F coincide at high energies. Thus, a curve corresponding to curve B can be calculated for this energy region where coincidence occurs.

[11] P. Axel, Brookhaven National Laboratory Report BNL-271, 1953 (unpublished).

From the difference in area between this latter curve and the observed pulse-height distribution, the high-energy porton of a curve corresponding to curve D of Fig. 2 can be constructed. Subtracting the area under this curve from the observed pulse-height distribution, the curve corresponding to curve C of Fig. 2 can be extended to lower energies. By utilizing this newly developed portion of this curve, the entire process was carried out repeatedly until the curve resembling curve B was constructed over the entire energy range. From this curve, a curve corresponding to curve A of Fig. 2 can be calculated. These data are shown as "experimental points" in Fig. 4. The calculated allowed spectrum for Ni^{59} is also shown. The areas under the array of points and under the allowed spectrum have been made equal on the energy interval extending from 100 kev to the end point of the spectrum. The ordinate values of the experimental points give the absolute quantum intensity along the spectrum. The measure of the absolute disintegration rate which is required to calculate the absolute gamma-ray emission will be described subsequently. The corrected observed emission is greater than the calculated absolute intensity of the allowed spectrum; therefore, it was necessary to multiply by 1.4 the ordinates of the allowed spectrum so as to equalize the area beneath it with that of the corrected observed distribution indicated by the points.

The theory of bremsstrahlung spectra of forbidden transitions has been investigated by Cutkosky,[12] who has shown that as in the case of beta spectra, the shape of the inner bremmsstrahlung spectrum is of importance. The factor by which the allowed spectrum must be modified to give the forbidden shape is of the form

$$C_{2s,T}(x)\sim x^2+\lambda(1-x)^2,$$

where x has been previously defined and

$$\lambda=\left[\frac{A_{ij}+(\alpha Z/R)(\frac{1}{2}T_{ij}+iR_{ij})}{A_{ij}+(\alpha Z/2R)(\frac{1}{2}T_{ij}+iR_{ij})}\right]^2.$$

The notation is that of Uhlenbeck and Konopinski.[13] The second forbidden spectrum corresponding to $\lambda=0.33$ is shown in Fig. 4 where the observed intensity at energies greater than 100 kev has been distributed according to the forbidden shape. If a pure tensor interaction is assumed, the value of A_{ij}/T_{ij} is found to be (-6). This result is to be compared with the positive values obtained from a study of negatron emitters.[14]

The spectrum of Ni^{59} was further investigated at quantum energies of less than 100 kev. An attempt was made to estimate self-absorption in the source by interposing additional absorbers of copper and extrapolating to zero absorber thickness. Because of the low counting rate, only qualitative results were obtained. It appears that the bremsstrahlung spectrum of Ni^{59} begins to increase in intensity at 40 kev and is continuing to rise at 25 kev.

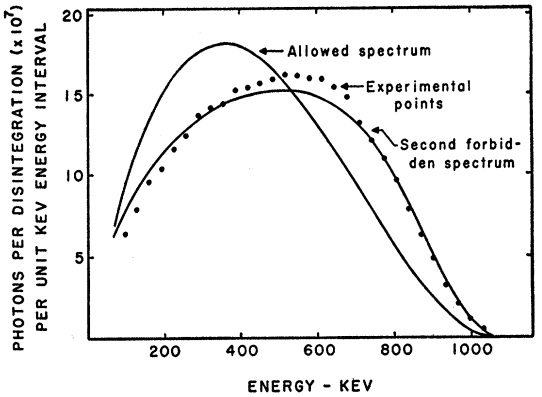

FIG. 4. The points give the observed gamma-ray distribution for Ni^{59} corrected for experimental effects. They are to be compared with an allowed spectrum of the form $x(1-x)^2$ and with the spectral shape to be expected for a second forbidden transition.

To obtain an estimate of the absolute intensity of the bremsstrahlung of Ni^{59}, it is necessary to measure the source strength, the number of electron capture disintegrations per unit time. A proportional counter was used for this purpose. This counter had a cylindrical aluminum cathode of diameter 7.6 cm, of length 30 cm, and of thickness 0.038 cm. The anode was of tungsten wire. A circular hole of diameter 1.27 cm in the center of the cathode served as a window. The cathode was fixed within a brass chamber and electrically insulated from it. This outer shell was so arranged that the radioactive source could be mounted within it and the distance between the source and the cathode window accurately adjusted. A small source of NiO (area 0.25 cm^2, weight 1.27 mg) was placed upon Scotch tape and covered with a thin film of formvar. The source was placed at a distance of 2 centimeters from the cathode opening. The gas filling of the counter was a mixture of argon and methane, the ratio of the partial pressures being 4:1. The total number of counts in the peak of the cobalt K x-ray line was recorded at several different pressures of the gas mixture. To calculate the total number of K-electron capture disintegrations per unit time, the following factors were taken into account: (1) the solid angle subtended at the source by the aperture in the cathode; (2) the fluorescence yield[15] of the K x-rays of cobalt; (3) absorption[16] of the x-rays of cobalt in the source of NiO; (4) escape of the K x-rays of argon; (5) absorption of the x-rays of cobalt in the gas mixture between the source and the window of the cathode; and (6) absorption within the counter, that is, the efficiency of the counter.

[12] R. E. Cutkowsky, Phys. Rev. **95**, 1222 (1954).
[13] G. E. Uhlenbeck and E. J. Konopinski, Phys. Rev. **60**, 308 (1941).
[14] D. C. Peaslee, Phys. Rev. **91**, 1447 (1953).
[15] E. H. S. Burhop, *The Auger Effect* (Cambridge University Press, Cambridge, 1952).
[16] A. H. Compton and S. K. Allison, *X-Rays in Theory and Experiment* (D. Van Nostrand Company, Inc., New York, 1935).

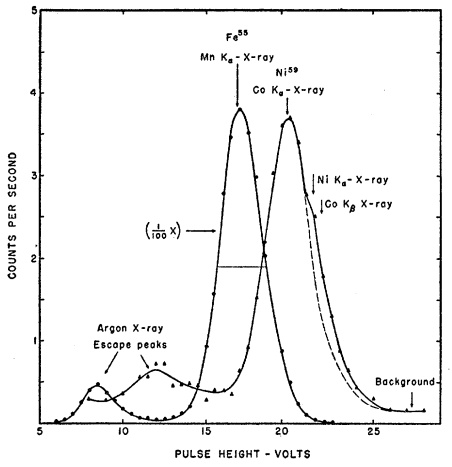

FIG. 5. Proportional counter spectra of the x-rays emitted in the decay of Fe^{55} and Ni^{59}.

The absorption coefficient of the counter mixture was determined for the manganese K x-rays in the studies of Fe^{55} to follow. The value of the absorption coefficient for the Co K x-rays was calculated from the simple equation

$$\mu_E/\mu_{E'}=(E'/E)^3,$$

where E and E' are the energies of the Co and Mn K x-rays.

The absence of any beta activity such as that of Ni^{63} is indicated by the curve of Fig. 5. No counts in excess of background were detected on either side of the Co x-ray at any of several gas pressures. Taking into account the variation of peak width with quantum energy, the peak corresponding to the x-rays of Co emitted in the decay of Ni^{59} is found to be somewhat wider than that to be expected when calculated from the width of the manganese x-rays. This additional width may result from the fact that the K_α and K_β lines of Co are more widely separated than are the K lines of Mn. With this consideration in mind, the intensity of any Ni K x-rays present is estimated to contribute less than 4% of the area under the x-ray peak. The K x-rays of Ni would be emitted in the course of absorption of the beta rays of any Ni^{63} which might be present in the thick source of NiO. From the Co x-ray intensity, the source strength of the 743 mg of NiO used in the gamma-ray measurements was estimated to be $(9.4\pm1.5)\times10^5$ disintegrations per second.

As previously indicated, the absolute probability of photon emission per disintegration per kev of quantum energy is shown in Fig. 4 in the energy interval extending from 100 kev to the end point. It has been estimated that systematic errors in the source strength determination and the absolute gamma-ray emission result in a probable error of 25% in the calculated probability of radiative capture. Thus, the ratio of the radiative capture probability in the second forbidden transition of Ni^{59} to the same probability for an allowed transition is 1.4 ± 0.4.

The half-life of Ni^{59} has been measured by several workers.[10,17] The reported values range from 7.5×10^4 to 8×10^5 years. Although in the present investigation the half-life measurement was not the purpose, from the data available in regard to neutron flux and capture cross section, the half-period was computed to be $(1.0\pm0.25)\times10^5$ years which agrees best with the value of reference 10.

ARGON-37

Gaseous A^{37}, produced by the $Ca^{40}(n,\alpha)A^{37}$ reaction, was obtained from Oak Ridge. The glass container was cylindrical in shape, of inner diameter 2 cm, of length 4 cm, with a break-off seal at one end. This source was placed at a distance of 3 cm from the surface of the crystal, and coaxially with the axis of the crystal.

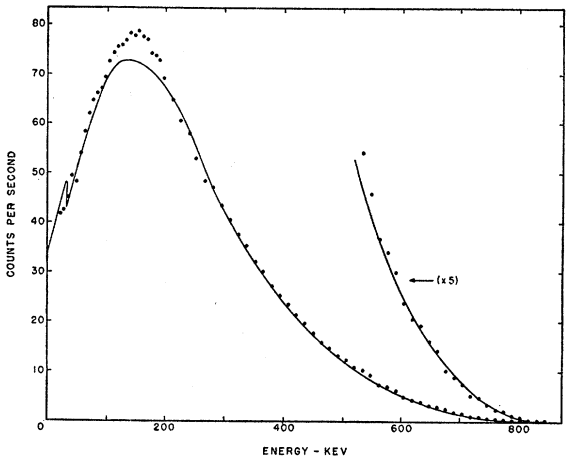

FIG. 6. The points are a plot of the observed pulse height distribution of A^{37}. The curve is of the allowed form $x(1-x)^2$, modified to take into account experimental effects.

The pulse-height spectrum, observed in the above described geometry, is shown in Fig. 6. It was necessary to consider the effect of the geometrical configuration of the source upon the detection efficiency. The variation of the counting rate with distance from the axis of the crystal in a plane 4 cm from the crystal surface was observed for a number of different quantum energies, and it was concluded that the variation of efficiency within the limits of the radius of the source and the energies contained in the spectrum of A^{37} is not more than 4%. Thus, to a first approximation, the source may be considered a line source extending from 3 cm to 7 cm before the crystal and on its axis. The efficiency of the crystal was calculated from the expression given earlier for values of point source distance of 0.0, 0.4, and 1–7 cm. The results are shown in Fig. 7 for gamma-ray energies of 150, 250, 400, 600,

[17] Hollander, Perlman, and Seaborg, Revs. Modern Phys. **25**, 497 (1953).

and 1000 kev. Because of the use of the graphical method of integration, the ordinates of the curves of Fig. 7 might be in error by as much as 2%. In Fig. 8 is shown the variation of the counting rate with the position of a point source on the crystal axis for the several quantum energies of Fig. 7. These curves are lettered A through E in order of decreasing quantum energy. These counting rates were obtained by multiplying the efficiency curves of Fig. 7 by the solid angle subtended by the crystal surface at the position of the source. Curve F shows the variation of solid angle alone with distance. The areas of Fig. 8 which are bounded by the counting rate curves, the distance axis, and the two ordinates at the source limits, are proportional to the integral values of the counting rates arising from a line source emitting gamma rays of the various quantum energies. The area bounded by curve F is proportional to the total intensity of radiation incident upon the crystal. The ratio of the area under any particular curve to the area under curve F gives the efficiency factor for any given quantum energy. The efficiency factor so calculated is shown in Fig. 9.

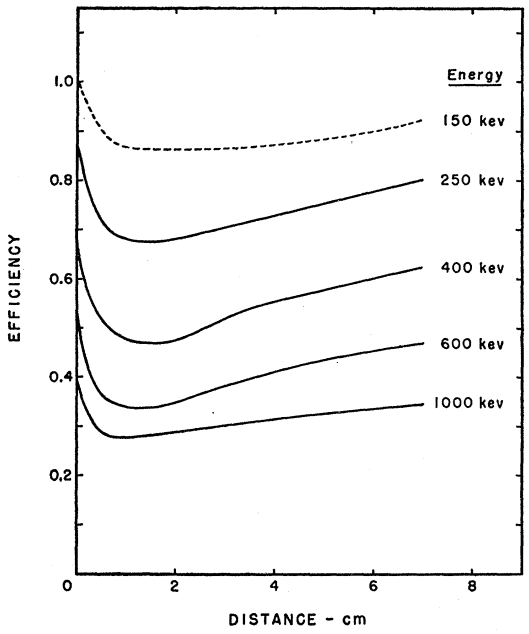

FIG. 7. Detection efficiency of the crystal of NaI(Tl) (diameter 3.5 cm, length 3.5 cm) as a function of the source distance along the axis of the crystal.

Modification of the theoretical spectrum of the form $x(1-x)^2$ and an end-point energy of 820 kev is shown in Fig. 10. The procedure followed in obtaining the various curves of Fig. 10 has been previously described in the discussion of the spectrum of Ni^{59}. The solid curve of Fig. 6 is a reproduction of curve F of Fig. 10. The ordinates of the curve have been determined by distributing the observed intensity between 200 kev and the end point according to the shape of curve F,

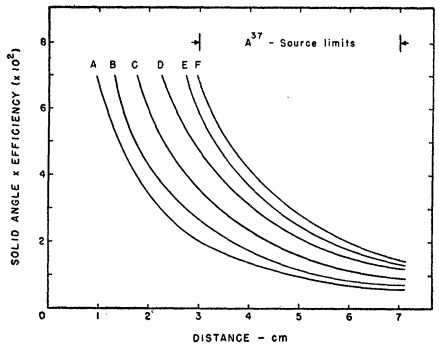

FIG. 8. Variation of the counting rate with distance (solid angle ×efficiency) for gamma rays of various energies: F, the solid angle itself; A, 1000 kev; B, 600 kev, etc.

Fig. 10. The agreement between the experimentally observed points and the modified theoretical curve is satisfactory. The excess over the theoretically expected values in the vicinity of 170 kev might be explained by (1) Compton scattering of photons by the glass envelope of the source, or (2) backscattering from the phototube and the surroundings. The spectrum was observed in the region of energy extending from 150 to 300 kev with addition of glass of a thickness about equal to that of the walls of the source containers. From these measurements, it was concluded that the effect (1) above must account for at least half the excess at low energies. Thus, it can be concluded that the quantum continuum of A^{37} is of the form $x(1-x)^2$ in the energy region extending from $\sim$35 kev to the end point.

The strength of the source of A^{37} was determined by a proportional counter. The active gas was diluted by inert argon to a pressure of 75 cm Hg in a volume of 2 liters. A small quantity of this mixture was admitted to a pressure of 1 mm into the proportional counter. The total pressure was subsequently increased to 40 cm Hg by addition of argon and methane. Counts corresponding in energy to the K and L x-rays of

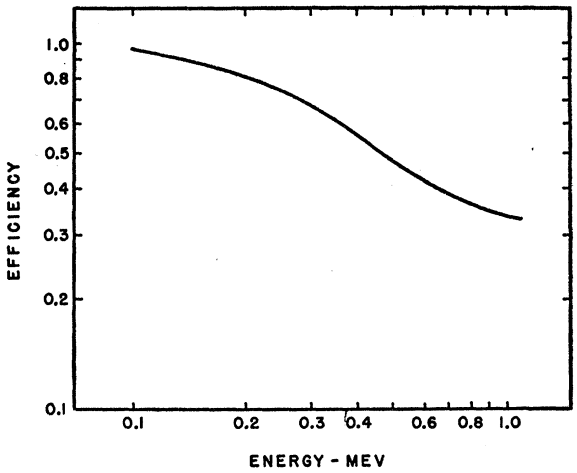

FIG. 9. Crystal detection efficiency for the distributed source of A^{37}.

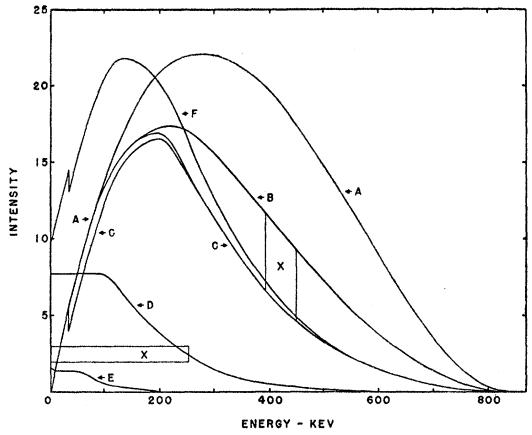

FIG. 10. Modification of the theoretically calculated spectrum for A^{37}, of form $x(1-x)^2$ and end point 820 kev.

chlorine were recorded. From a consideration of the absorption coefficient of argon for these x-rays, it was possible to conclude that the counting rate arose almost entirely from Auger electrons. The results were corrected for the fluorescence yield (0.92). To correct for end effects of the sensitive volume of the counter, the counting volume was separated into two parts by dividing the wire into two parts held together by a small glass bead. The ratio of the two volumes so created was 2:1. End effects were eliminated by taking the difference count of the two sections. The source strength obtained from the measurements described above was $(2.1\pm0.2)\times10^8$ disintegrations per second. From this measurement and estimates of the absolute gamma-ray intensity, the ratio of the observed probability of emission to the theoretical value, in the region of agreement is calculated to be $P_{(\text{exp})}/P_{(\text{theoret})}=1.05\pm0.25$.

In a recent investigation,[18] Lindqvist and Wu have also noted good agreement between the observed spectrum of A^{37} and the theoretical calculations.

IRON-55

A source of Fe^{55} was obtained from Oak Ridge. The sample was converted to Fe_2O_3 (about 5 mg in weight), deposited upon a thin film of mica, and covered over with formvar. At the time of the measurements, the source was approximately one and one-half years of age and contained no detectable trace of Fe^{59}. The radioactive material was placed at a distance of one centimeter from the surface of the crystal and on its axis. The experimentally measured points are shown in Fig. 11. They have been corrected for resolution, efficiency of the crystal in the geometry employed, iodine K x-ray escape, and absorption of the soft quanta in Al_2O_3 and Be. The correction for Compton effect is negligible for the quantum energies emitted in the decay of Fe^{55}. The theoretically calculated spectrum of Glauber and Martin[9] is represented by the solid curve which is seen to be in excellent agreement with observation at energies greater than 100 kev. At lower energies, the measured spectral intensity is lower than calculated. This reduction may be related to the effect of screening upon p-electron capture as has been suggested.[9]

The strength of the source of Fe^{55} was measured in a manner described in the case of Ni^{59}. A strong source of Fe^{55} was mounted in the side of the counter, at a distance of 7.6 cm from the cathode entrance. The counts arising from the K x-rays of Mn were recorded as a function of the gas pressure. The number of x-ray counts detected in such a geometry is given by the expression

$$N=N_0e^{-\mu dl_1}(1-e^{-\mu dl_2}),$$

where μ is the mass absorption coefficient, d the density of the gas, l_1 the length of the entrance channel of the counter, l_2 the diameter of the counter, and N_0 the number of photons emitted in the solid angle subtended at the source by the aperture of the counter. For the geometry employed, $l_1=l_2=7.6$ cm. The counting rate will be a maximum when

$$\mu dl_1=\log_e 2.$$

Thus, μ could be determined.

After the measurement described in the foregoing, and after all gamma-ray studies had been completed, the source of Fe^{55} was dissolved in HCl and diluted to a volume of 5 cc. A carefully measured volume of 0.2 cc of this solution was used as a small source of Fe^{55}. This source was mounted at a distance of 3.5 cm from the aperture in the cathode of the counter, and the counting rate was observed at various pressures. Thus, the source strength could be calculated. The total source strength was found to be 7.2×10^7 disintegrations per second. In the region of agreement of the theoret-

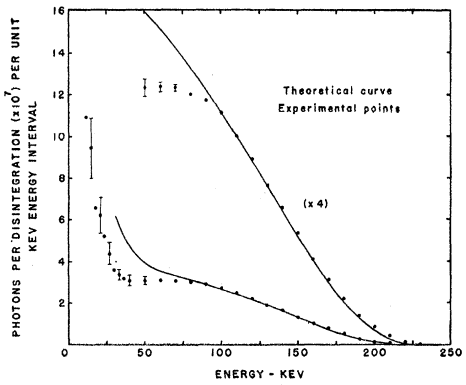

FIG. 11. Observed pulse-height spectrum of Fe^{55} (points) corrected for experimental effects. The curve is the theoretically calculated spectrum of Glauber and Martin.

[18] T. Lindqvist and C. S. Wu, Phys. Rev. **98**, 231(A) (1955); **100**, 145 (1955).

ical curve with the experimental points, the ratio of the observed radiative capture probability to the theoretically calculated one was found to be 1.10 ± 0.25.

ACKNOWLEDGMENTS

The writer wishes to express appreciation for the kind interest of Dr. C. E. Mandeville who prepared this manuscript for publication. Useful discussions with Dr. F. R. Metzger are also gratefully acknowledged. The various chemical purifications were performed by Dr. W. B. Keighton of Swarthmore College. The author wishes to further express appreciation for the award of a fellowship by the Bartol Research Foundation, and to Dr. W. F. G. Swann for encouragement.

PHYSICAL REVIEW VOLUME 102, NUMBER 2 APRIL 15, 1956

Elastic Scattering of 340-Mev Protons by Deuterons*

OWEN CHAMBERLAIN AND DAVID D. CLARK†
Department of Physics and Radiation Laboratory, University of California, Berkeley, California
(Received December 19, 1955)

The differential cross section for the elastic scattering of 340-Mev protons by deuterons has been measured at eight angles from 30° to 150° in the center-of-mass system. A coincidence counting system using scintillation counters detected both product particles, the elastic effect being separated from the inelastic through identification of the scattered deuterons by photographically recorded pulse heights produced in a counter telescope. The resulting cross section is, at 30°, 2.2 mb/steradian; 40°, 0.89; 50°, 0.39; 70°, 0.11; 90°, 0.047; 110°, 0.042; 130°, 0.047; and 150°, 0.099, in center-of-mass units. The total (statistical and systematic) errors range from 15 to 24%. The total elastic cross section is estimated to be 6.0 ± 1.2 mb. Problems of interpretation using the impulse approximation are discussed; the sticking factor is calculated for three different *n-p* potentials. At scattering angles of 30° and 40° there appears to be very little interference effect between *n-p* and *p-p* scattering. The interference is perhaps slightly destructive.

I. INTRODUCTION

THE role of nucleon-deuteron scattering in the attempt to learn more about nuclear forces is threefold. First, it gives data on the scattering of nucleons by a simple nuclear system. Second, we expect that between the scattered waves from the two components of the deuteron there will be interference effects that will give us information as to the relative phases of the nucleon-nucleon scattering amplitudes. Third, as targets consisting of neutrons do not exist, neutron-deuteron scattering is our closest approach to *n-n* scattering, and a comparison of *n-d* and *p-d* scattering can answer the question of whether or not nuclear forces are charge-symmetric. Moreover, though nucleon-deuteron scattering is a three-body problem, theoretical treatment—at least for small angles of deflection—is possible at the higher energies by use of the impulse approximation.

Experimental work to date in the higher energy region has been that of Ashby[1] (32-Mev *p-d* scattering; 21 Mev available in the center-of-mass system); Chamberlain and Stern[2] (192-Mev *d-p*; 63 Mev in c.m. system); Cassels, Stafford, and Pickavance[3] (145-Mev *p-d*; 95 Mev in c.m. system); and Schamberger[4] (240-Mev *p-d*; 156 Mev in c.m. system). The 90-Mev *n-d* (59 Mev in c.m. system) case has been studied both by Powell[5] with cloud-chamber techniques and very recently by Youtz[6] with counters. The pick-up region (near 180°) of *p-d* scattering has been the subject of Bratenahl[7] at energies from 95 to 138 Mev, and of Teem and Kruse[8] at 95 Mev.

The experiment described here was undertaken because of the usefulness of any additional high-energy scattering data, and in particular because the impulse approximation becomes increasingly valid with higher energy. The proton beam energy used was 340 Mev, the available energy in the center-of-mass system being 218 Mev.

II. GENERAL METHOD

The process of measuring the cross section consisted of the measurement of the four quantities: $D(\Theta)$, the number of elastic *p-d* scattering events observed per

* This work was performed under the auspices of the U. S. Atomic Energy Commission. A portion of this research was submitted as a thesis by one of us (D.D.C.) in partial satisfaction of the requirements for the Ph.D. degree at the University of California.

† Now at Department of Engineering Physics, Rockefeller Hall, Cornell University, Ithaca, New York. For the major portion of this research, a U. S. Atomic Energy Commission predoctoral fellow.

[1] V. J. Ashby, University of California Radiation Laboratory Report UCRL-2091 (unpublished).

[2] O. Chamberlain and M. O. Stern, Phys. Rev. **94**, 666 (1954).

[3] Cassels, Stafford, and Pickavance, Nature **168**, 468 (1951).

[4] R. D. Schamberger, Phys. Rev. **85**, 424 (1952).

[5] W. Powell, University of California Radiation Laboratory Report UCRL-1191 (unpublished).

[6] B. L. Youtz, University of California Radiation Laboratory Report UCRL-2307 (unpublished).

[7] A. Bratenahl, University of California Radiation Laboratory Report UCRL-1842 (unpublished); Phys. Rev. **92**, 538(A) (1953).

[8] J. M. Teem and U. E. Kruse, Phys. Rev. **95**, 664(A) (1954).